

# Development of the PERC Solar Cell

Andrew Blakers 

**Abstract**—This paper reviews the development of the passivated emitter and rear cell (PERC) silicon solar cell in the 1980s, which set several efficiency records, but was not taken up commercially at the time. Following extensive development of suitable fabrication processes, materials, and production tools, the PERC solar cell is now on track to become the dominant commercial solar cell. Since photovoltaics (PV) itself is on track to become the dominant energy generation technology, the PERC is having a global impact in both energy generation and greenhouse gas emission reduction. Assuming an average growth rate of annual PV installations of 25%, PV mitigation of greenhouse gases will reach about 5% in 2022, including 2% from PERCs, with much higher values expected later in the 2020s. This review focuses on the period of development of the PERC during the 1980s.

**Index Terms**—Passivated emitter and rear cell (PERC), photovoltaics (PV), silicon solar cell.

## I. INTRODUCTION

**I**N 2017, solar photovoltaics (PV) constituted 40% of global net new electricity generation capacity additions with fossil, nuclear, wind, hydro, and other renewables constituting the balance (see Fig. 1). PV is growing much faster than the other generation technologies and may exceed half of global net new generation capacity annual additions by 2020.

Continued rapid growth of PV (and wind energy) would have a major impact on global emissions of greenhouse gases by displacing coal and gas electricity generation. The average growth rate of PV in terms of annual new deployment has been about 30% per year over the past ten years [1]. This growth rate, if continued until 2025, would result in PV producing 10% of the world's electricity.

For decades, about 90% of global solar cell production has been of the aluminum back surface field (Al-BSF) design. This cell design offers moderate efficiency and simple and reliable fabrication, and utilizes vast experience in terms of manufacturing tools, materials, and procedures.

The cell manufacturing cost (separate from polysilicon and wafering) represents about one-quarter of the module cost, while the module cost is about one-half of the system cost [8]. Thus, the cell fabrication process is about one-eighth of the completed system cost. Most module and system costs depend upon the area of cell deployed and, hence, depend inversely on cell efficiency.

Manuscript received December 15, 2018; revised February 2, 2019; accepted February 8, 2019. Date of publication February 26, 2019; date of current version April 19, 2019.

The author is with the Australian National University, Canberra, ACT 0200, Australia (e-mail: andrew.blakers@anu.edu.au).

Digital Object Identifier 10.1109/JPHOTOV.2019.2899460

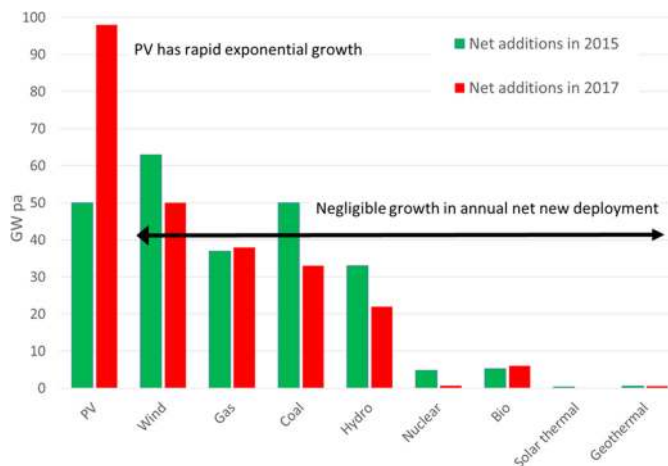


Fig. 1. PV has experienced sustained rapid exponential growth over decades, while other generation technologies are currently experiencing static or negligible sales [1]–[7].

The cost of a solar cell as a proportion of the cost of a complete PV system continues to fall. This is because most system components (such as transport, land, fencing, steel support structures, wiring, aluminum frames, and glass) have greater commercial maturity than the solar cell and, hence, have fewer opportunities for price reduction. This places a premium on cell efficiency, since an increase in cell efficiency leverages cost reductions across most of the value chain by reducing the area of components that needs to be deployed for a given power rating. In contrast, a corresponding decrease in cell cost in terms of dollars per square meter has substantially less impact.

Approaches such as back contact cells and heterojunctions offer high performance for commercial cells (approaching 25% efficiency) albeit at relatively high cost and requiring substantial changes to standard industrial cell processing technology. The passivated emitter and rear cell (PERC) design offers current and future commercial cell efficiency in the range 21–24% [8] and requires relatively few changes to standard Al-BSF processing. This allows existing industrial equipment, materials, and processes to continue to be used.

The PERC solar cell design is rapidly gaining market share in the PV industry. The main motivation for the shift to the PERC is improved efficiency compared with the incumbent Al-BSF cell. The major advantages of the PERC over the Al-BSF cell are reduced rear-surface recombination and improved rear-surface reflectivity. According to the International Technology Roadmap for PV, the PERC constituted 20% of the PV industry in 2017 and will reach 50% of the global PV industry in the 2020s (see Fig. 2) [8].

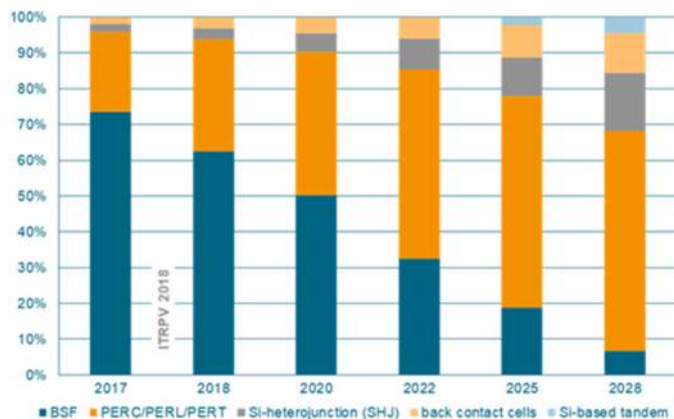


Fig. 2. Worldwide market shares for different silicon cell technologies. Reprinted from [8].

A move from reliance on 18–19% efficient Al-BSF multicrystalline solar cells in 2017 to 22–24% efficient monocrystalline PERCs in 2025 offers an efficiency increase of one-quarter, which translates to a substantial decrease in the price of electricity from large-scale PV systems.

In 2017, PERC sales were about 20 GW, which constituted about 8% of global net new generation capacity additions from all sources. Cumulative sales of PERC modules to the end of 2017 were about 37 GW with a value of about US\$16 billion. These calculations draw upon historical volume and price data for PV and the PERC sales fraction [8]. Much larger PERC fractions and cumulative sales could occur in the near future.

At the end of 2017, PERC modules were mitigating about 60 million tons of CO<sub>2</sub> emissions per year (about 0.16% of the global total) through displacement of coal burning. This rough estimation assumes annual PV output of 1500 kWh per kilowatt installed (averaged across rooftop and ground-mounted systems) and displacement of coal that has an average emission intensity of 1 t of carbon dioxide per megawatt-hour. The PV industry as a whole is currently mitigating about 2% of global greenhouse gas emissions, and the wind energy industry is mitigating 3%. Assuming an average growth rate of annual PV installations of 25%, PV mitigation will reach 5% in 2022, including 2% from PERCs, with much higher values expected during the 2020s.

In light of the global impact of the PERC solar cell design, it is interesting to review the development of PERCs at the University of New South Wales (UNSW) in Australia during the 1980s.

## II. DEVELOPMENT OF THE PASSIVATED EMITTER AND REAR CELL

The 1980s was a period of steady improvement in silicon solar cell performance in several research laboratories. UNSW entered the field following work to develop metal–insulator–semiconductor (MIS) solar cells by Green and Godfrey [9]. The key feature of the MIS cell is continuous passivation of the upper surface including under the metal contacts via a thin oxide that allows tunneling of current between the wafer and the metal

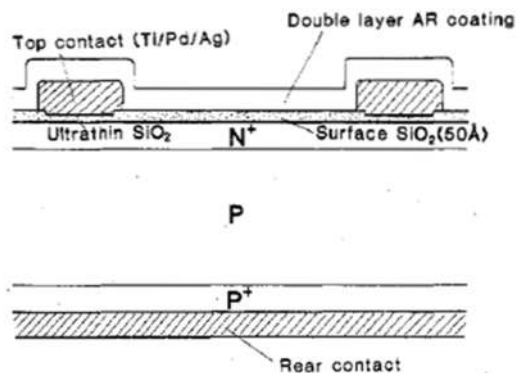


Fig. 3. Cross section of the reported 18% efficient solar cell. Reprinted from [11].

contact. A  $V_{oc}$  of 678 mV (AMO, 25 °C) was reported by Blakers and Green in 1981 [10] for a cell that used a combination of an MIS contact and a light surface phosphorus diffusion (“metal-insulator-N-P (MINP)”).

An 18% efficient cell was reported by Blakers *et al.* in 1984 [11]. Features of the cell were a 0.1–0.2- $\Omega \cdot \text{cm}$  p-type float-zone substrate, light phosphorus diffusion (>100  $\Omega$  per square), passivation of the top surface of the cell with thermal oxide, reduced optical reflection losses by using a double-layer antireflection coating (ZnS/MgF<sub>2</sub>), and silver electroplating to reduce resistive losses in the cell. The cell had a polished front surface. In order to reduce recombination at the front metal contact (Ti/Pd/Ag), the cell used the MINP design and had a moderate contact area (4.6%). The rear surface comprised an alloyed aluminum layer. Fig. 3, taken from the original paper, shows the cell in cross section. The  $V_{oc}$  was 643 mV at 28 °C.

An improvement to 19% efficiency was reported soon afterwards by Green *et al.* [12] for cells independently measured at the Solar Energy Research Institute (SERI, the forerunner of the National Renewable Energy Laboratory). Cell design was similar, and efficiency improvement came from tweaking the cell fabrication process. The best cells dispensed with the MIS contact because the oxide layer added to process complexity but did not increase efficiency (at this modest  $V_{oc}$ ). The acronym “PESC” (passivated emitter solar cell) was introduced. The top metal contact fraction (around 1%) was lower than in the 18% MINP cell, and the  $V_{oc}$  was a little higher at 653 mV. Both the MINP and PESC design reached a  $V_{oc}$  of 690 mV (AMO, 25 °C) in test cells.

Addition of photolithographically defined micro grooving to reduce front surface reflection and introduce light trapping resulted in the first report of a 20% efficient cell by Blakers and Green [13] in 1986. Fig. 4, taken from the original paper, shows the cell in cross section. The SERI measured the cell as 20.9% efficient with a  $V_{oc}$  of 661 mV at 28 °C.

Development of high-efficiency cells at UNSW was guided by a philosophy of “improve the  $V_{oc}$  first and the current and fill factor will follow.” Passivation of the front surface suppressed recombination and allowed voltages to rise. Minimization of recombination at the front metal contact was achieved by variously minimizing the contact area, by interposing a thin passivating

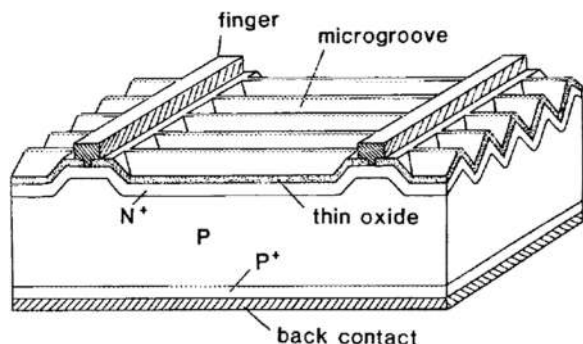


Fig. 4. Cross section of the first reported 20% efficient solar cell. Reprinted from [13].

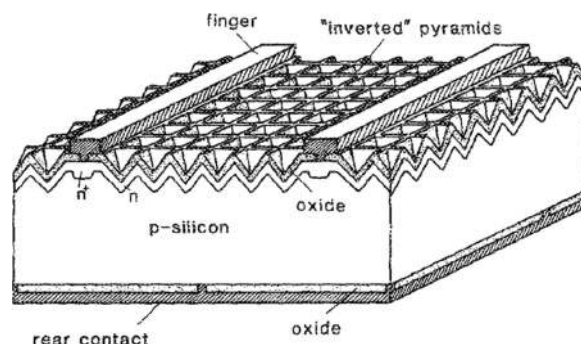


Fig. 5. The PERC cell. Reprinted from [16].

tunnel oxide between the silicon and metal, and by diffusing the region beneath the metal. The area between the metal fingers (about 99% of the front surface) was passivated with a thermal oxide, which also prevented the silver-plating on the fingers (which spilled out beyond the contact openings as illustrated in Fig. 4) from contacting the silicon.

As  $V_{oc}$  rose above 650 mV, demonstrating that the front surface passivation was effective and that minority carrier diffusion lengths were comparable with the wafer thickness, attention turned to minimizing recombination at the rear surface. The rear surface of these early cells comprised alloyed aluminum—a so-called back surface field (BSF). It was known (by analogy with the front surface) that oxide passivation (rather than metallization) of most of the rear surface would reduce recombination. Thus, the Al-BSF layer on the rear surface was recognized as limiting progress toward higher cell efficiency because of high recombination rates and poor reflectivity.

The aluminum–silicon alloy is a good gettering layer, which was important for coping with poor cleanliness in diffusion and oxidation furnaces. Typically, the alloying occurred simultaneously with the passivation oxidation for the front surface. Importantly, deletion of the aluminum alloying step caused reduced cell performance due to degradation of the minority carrier lifetime during furnace steps.

Reducing the metal–silicon contact area on the rear would reduce rear-surface recombination, by analogy with the low-area metal contact on the front surface. A bifacial design in which the rear metal is restricted to 5–10% of the surface, with a passivation dielectric covering the rest of the rear surface, was one possibility. Another was to extend the rear metal across the entire rear surface to create an effective mirror, but to restrict the metal contact fraction by including a passivation dielectric between the silicon and the aluminum. The overlap of plated silver over the passivation oxide on the front surface (see Fig. 4) partially used this concept. The optical advantage of a high-quality rear-surface mirror was appealing.

The introduction of chlorine processing to UNSW for contamination control, initially using compressed HCl and later using 111 trichloroethane [14], was important because high minority carrier lifetimes ( $\sim 1$  ms) could then safely and reliably be achieved without the use of rear-surface aluminum alloy gettering.

In 1988, promising cells with the PERC structure were developed, and cell efficiencies of 22–23% were reported by Blakers *et al.* in 1989 [15]–[18]. The PERC acronym was introduced as an extension of the previous PESC acronym. The distinctive feature of PERCs is the rear surface, where optical and recombination losses were greatly reduced compared with BSF cells by using an aluminum reflector atop a rear passivation dielectric. Contact between the silicon and aluminum was achieved via an array of small holes in the dielectric covering about 1% of the rear surface with spacing of around 1 mm. The rear contact fraction and spacing is a tradeoff between recombination and resistance losses. Fig. 5 taken from an original paper shows the PERC in cross section. This simple structure is capable of high efficiency.

In the early PERCs, a thermal passivating oxide was grown on the rear surface, and an array of small holes were opened using photolithography. Aluminum was then evaporated onto the rear surface followed by sintering in forming gas at 250–400 °C.

Inverted pyramids (via photolithography) and random pyramid texturing were introduced to reduce reflection losses compared with micro grooves at the nontextured “ridge-tops” of the grooves, and to improve light trapping due to scattering of light by pyramid facets into the third dimension.

The front surface included a selective phosphorus emitter (heavier beneath the metal contacts), antireflection coating, and thermal oxide passivation. Oxide passivation of the front and rear surface was improved by aluminum annealing or wet forming gas annealing at 400 °C, and the best voltage observed was 705 mV.

The initial high-performance PERCs had no p+ layer at the rear contact points. This was a simple design that took advantage of the fact that nonalloyed aluminum can make low resistance contact directly to a low-resistivity p-type wafer ( $0.1$ – $0.5 \Omega \cdot \text{cm}$ ) without surface diffusion, whereas similarly doped n-silicon is difficult to contact so simply. A rear contact fraction in the range 0.1–10% worked well for low-resistivity p-type silicon and was later refined using spreading resistance calculations.

The simplicity and speed of the PERC fabrication process was important—it allowed rapid progress to be made. It was soon obvious that the PERC could produce high open-circuit voltage and was better than alternatives, and a team of six people began working on the cell.



In some cells, the aluminum was alloyed into the silicon at the rear point contacts at temperatures above 600 °C. However, the results without alloying were better, and this approach was not continued. Problems encountered included voids and damage to the rear oxide. Later work by many others has resulted in a commercially feasible method of implementing this approach, as described in Section IV.

It was clear that including a boron diffusion at the back surface had the potential to further improve cell performance, albeit at the expense of added complexity. Boron diffusions (from solid sources, spin-on films, and boron tribromide) covering a few percent (passivated emitter, rear locally diffused—“PERL”) or the entire rear surface (passivated emitter, rear totally diffused—“PERT”) were explored during 1988. At the time, there was insufficient knowledge at UNSW of techniques to preserve minority carrier lifetime during boron diffusion, and cell performance was slightly below cells without boron diffusion.

Some cells were made using n-type substrates with an MIS contact at the rear with indifferent results. The great convenience of using a well-understood and reliable phosphorus diffused emitter on a p-substrate would have to be eschewed in favor of a boron-diffused emitter on an n-substrate. For this reason, the focus remained on p-type substrates, which the PV manufacturing industry has favored throughout its history.

In the 1990s, further improvements to PERL and PERT laboratory cells were made at UNSW, leading to cells in the 24–25% efficiency range, by the authors of [19]–[23]. These cells featured excellent light trapping and reflection control, optimized grid design to maximize the fill factor, excellent surface passivation, and high minority carrier lifetimes. The silicon solar cell efficiency record remained at UNSW until recently.

### III. INTERDIGITATED BACK CONTACT AND BIFACIAL SOLAR CELLS

The work at UNSW was paralleled by work elsewhere covering improved surface passivation, cell design, and other features. The UNSW group benefited substantially from concurrent work in developing bifacial and interdigitated back contact (IBC) cells.

In 1985, a startling  $V_{oc}$  of 720 mV was achieved in a test structure comprising a 50- $\mu\text{m}$ -thick 0.5- $\Omega\cdot\text{cm}$  p-type wafer passivated with a mixture of silicon dioxide and microcrystalline silicon [24]. The p-contact was made with Ga–In metal at the edge of the wafer. This demonstrated that much higher cell efficiencies were possible than hitherto demonstrated.

Cuevas has reviewed the development of bifacial solar cells [25]. An innovation reported in 1977 by Chevalier and Chambouleyron was a device in which the rear metal grid made contact to the substrate, while the rest of the rear surface was passivated (and unmetallized) [26]. Notable contributions to bifacial cells including rear-surface diffusions and improved cell efficiencies came from the University of Madrid [27], [28], the Fraunhofer Institute for Solar Energy Systems, Comsat, Solarex, and AEG Telefunken. In 1988, Knobloch *et al.* reported bifacial cell test structures with a widely spaced

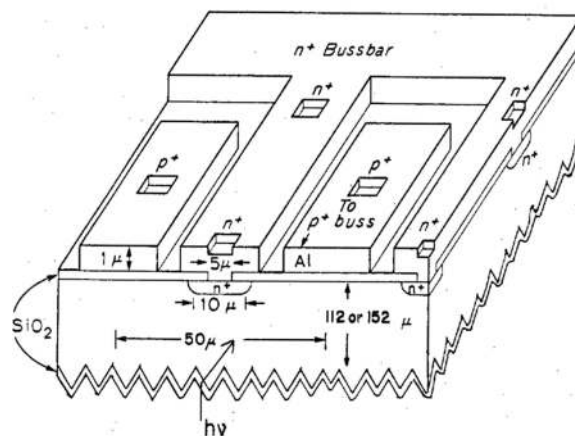


Fig. 6. IBC cell. Reprinted from [32].

rear-surface grid that included a local BSF beneath the grid with surface passivation elsewhere [29].

Novel MIS structures and the use of charged dielectrics (aluminum oxide and silicon nitride) for low-temperature surface passivation were investigated by Hezel and Jaeger [30]. These films have found widespread application and were applied to PERC and other cells at the Institute for Solar Energy Research with good results [31].

Research groups, particularly those from Stanford University and the University of Louvain, developed excellent IBC silicon solar cells during the 1980s, primarily for concentrator applications [32]–[35]. Both contact polarities were located on the rear surface (see Fig. 6) to eliminate obscuration of light (which is helpful for a concentrator cell). These groups faced similar problems to the UNSW group, and the device designs converged in many respects.

These IBC cells featured excellent surface passivation on both surfaces, boron and phosphorus point-contact (small-area) diffusions for electrical contact, lightly doped substrates, high minority carrier lifetimes, surface texturing for reflection control and light trapping, and reflection of infrared light by the rear-surface metallization. Cell efficiencies of 22% (with  $V_{oc}$  of 681 mV) under one-sun illumination and 27.5% under concentration were reported in 1986 [32]. In 1989, the SERI confirmed one-sun efficiency of 22.3% and  $V_{oc}$  of 703 mV for an IBC cell [34]. The IBC cell fabrication process used in this research was complicated. Subsequently, a simplified version was developed and commercialized for nonconcentrator applications by the SunPower company.

Good control over device processing and detailed characterization allowed the Stanford group to adapt IBC cells to have metal contacts on both surfaces (see Fig. 7). In 1990, bifacially contacted cells with an efficiency of 22% and  $V_{oc}$  of 700 mV under one-sun illumination, and 26% under concentration, were reported [36].

### IV. COMMERCIAL PASSIVATED EMITTER AND REAR CELLS

Many of the materials and processes used in laboratory PERCs were unsuitable for commercial production. A period of

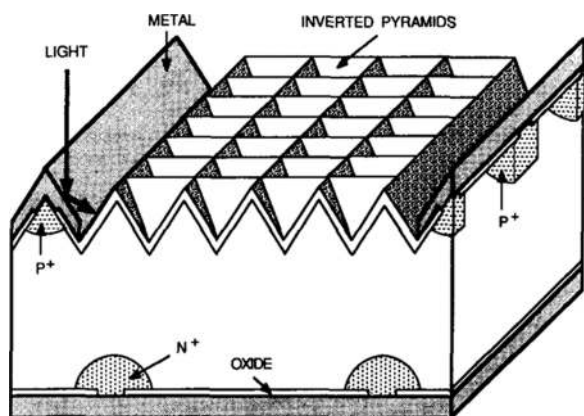


Fig. 7. Adaptation of IBC cells to bifacial metal contacting. Reprinted from [36].

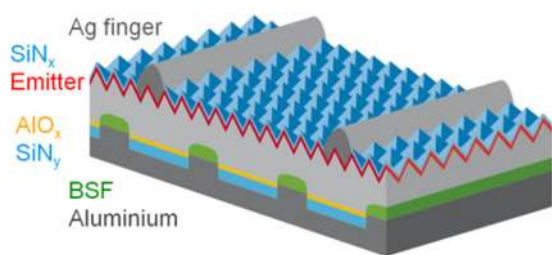


Fig. 8. Typical commercial PERC solar cell with  $\text{AlO}_x/\text{SiN}_y$  rear passivation and local screen-printed Al rear contacts formed by laser-opening of the rear dielectric. Reprinted from [38].

25 years elapsed between the first laboratory cells and the first substantial production of PERCs. During this period, most commercial solar cells were fabricated on p-type silicon substrates with an alloyed aluminum rear surface—the Al-BSF approach.

Centrotherm announced its Centaurus PERC in 2011 featuring a local Al-BSF rear contact, PECVD passivation layer deposition on the rear surface, laser patterning, and efficiencies above 19% for 156-mm-diameter wafers [37]. Importantly, “an easy integration in existing and future production technology was a main precondition” for the design of the Centaurus cell.

Several variations of the PERC are now under commercial production. This has been achieved through contributions from many people and companies to materials, process techniques, and production machinery. Dullweber and Schmidt have published an excellent review of the development of commercial PERCs [38]. Liu *et al.* [39] have recently reviewed high-efficiency cell designs, and Schmidt *et al.* [40] have reviewed developments in surface passivation. Key points relating to the development of commercial PERCs are described here in summary only. Refer to [38] for a detailed review including original references.

A typical commercial PERC is illustrated in Fig. 8. The substrate is boron-doped (p-type) single- or multicrystalline silicon. The front surface has texturing, phosphorus diffusion, screen-printed silver fingers, and a silicon nitride ( $\text{SiN}$ ) layer. The  $\text{SiN}$  layer is simultaneously an antireflection coating and a passivation coating for the region between the silver fingers. This front surface design is similar for both Al-BSF and PERCs, which avoids the need to develop new tools, materials, and processes.

Solar cells made using thick wafers with poor minority carrier diffusion lengths (less than the wafer thickness) do not benefit significantly from improved rear-surface passivation. In recent years, there has been steady progress in improving wafer quality and reducing wafer thickness, including through the shift to diamond wire sawing and increasing use of high-quality Czochralski monocrystalline silicon wafers. The rear-surface passivation and improved optical reflectivity provided by the PERC design now makes a significant difference (around 1.5% absolute [8]) to cell performance compared with the Al-BSF design. This gap is expected to widen.

The early PERC laboratory cells explored several methods for making electrical contact between aluminum and silicon at the rear surface, including nondoped low-temperature direct contact (sintered at 300–400 °C), alloying the aluminum (at 600–800 °C) and boron diffusions [either at the point contacts (PERL), or across the entire rear surface (PERT)]. Of these, alloying the aluminum proved to be most commercially effective.

The rear surface of the Al-BSF cell comprises alloyed aluminum with relatively poor passivation quality and optical reflectivity. In contrast, the PERC design features a screen-printed aluminum layer that makes periodic alloyed contact with the silicon surface. Between these regions is a dielectric layer, typically aluminum oxide and silicon nitride, that passivates most of the rear surface and also prevents the aluminum from touching the silicon except in the contact regions (see Fig. 8). Thus, the PERC design offers reduced rear-surface recombination and improved rear-surface reflectivity.

The original PERCs had  $\text{SiO}_2$  dielectric passivation on the rear surface. This can be problematical for commercial production for several reasons: the positive charges generally found in  $\text{SiO}_2$  can cause a depletion region or an n-type inversion layer to appear at the rear surface, which has the effect of increasing rear-surface recombination;  $\text{SiO}_2$  by itself cannot readily withstand the firing step for the overlying screen-printed aluminum paste; and high temperature thermal oxidation can cause lifetime degradation in some substrates. Several methods have been developed to overcome these problems, including the use of  $\text{AlO}_x/\text{SiN}_y$ . The  $\text{AlO}_x$  contains negative charges, which causes accumulation of holes and depletion of electrons at the rear surface, which assists with rear-surface passivation;  $\text{SiN}_y$  is a tough dielectric that can withstand the firing step for the screen-printed aluminum paste. While  $\text{SiN}_y$  is already widely used on the front surface of silicon solar cells, commercial deposition of  $\text{AlO}_x$  required the development of new tools.

Opening contact windows in the rear-surface dielectric in laboratory PERCs was by photolithography, which is expensive. The development of high-speed laser ablation of the rear dielectric to make contact opening allowed low-cost rear-surface patterning. Substantial work was required to develop suitable high-speed tools and processes.

The phosphorus diffusion step in production of Al-BSF cells typically dopes both front and rear surfaces. The subsequent aluminum alloying at the rear surface overrides the rear-surface phosphorus doping. In a PERC, only local aluminum alloying takes place and so phosphorus doping must be excluded at the rear surface. Commercial processes were developed to deposit

a protective dielectric on the rear surface prior to phosphorus diffusion or to selectively remove the rear phosphorus layer postdiffusion using a single-sided wet etching process.

The rear metal in laboratory PERCs was evaporated aluminum, which is not an economic proposition. Its replacement by screen-printed aluminum, similar to the Al-BSF cell, allowed continued use of a leading low-cost mass-production technique.

Silicon and aluminum forms a eutectic alloy in the contact openings during the firing step, and a thin aluminum doped region can form at the interface between the eutectic alloy and the bulk of the silicon wafer. This reduces contact resistance and recombination at the contact points. Considerable work was required to reliably form aluminum alloy contacts, including the development of specialized metal pastes.

## V. CONCLUSION

The development of the PERC built upon earlier work at UNSW and elsewhere in the development of high-efficiency silicon solar cell technology. The parallel development of high-performance IBC and bifacial cells shared many features in common, including high-lifetime wafer processing, dielectric passivation of most of both cells' surfaces, small-area metal contacts, and rear-surface reflectors.

There was a 25-year gap between development of the PERC and its widespread commercial adoption. Strong drivers for more efficient cells have recently arisen due to the falling share of cell costs as a proportion of total PV system costs. Techniques that allowed low-cost commercial fabrication of PERCs were developed during the intervening years by many people and companies. The closeness of the current PERC process and the older Al-BSF process has allowed a smooth and rapid commercial transition to the PERC.

## ACKNOWLEDGMENT

In reviewing development of the PERC in the 1980s and 1990s, a gratifying feature is the number of people at UNSW who were acknowledged by way of authorships to have made significant contributions. Twelve people contributed substantially to the high efficiency cell program, including 6 people who made substantial contributions to the development of the PERC. Discussions with C. Ballif, A. Cuevas, J. Schmidt, M. Stocks, and P. Verlinden are gratefully acknowledged, as are the formal reviewers. Opinions expressed in this paper are the responsibility of the author.

## REFERENCES

- [1] IRENA Capacity Statistics, 2018. [Online]. Available: <http://www.irena.org/publications/2018/Mar/Renewable-Capacity-Statistics-2018>
- [2] Ren21 Annual Report, 2018. [Online]. Available: <http://www.ren21.net/>
- [3] Global Trends in Renewable Energy Investment, 2018. [Online]. Available: <http://fs-unep-centre.org/sites/default/files/publications/gtr2018v2.pdf>
- [4] World Nuclear Association, 2018. [Online]. Available: <http://www.world-nuclear.org/information-library/facts-and-figures/world-nuclear-power-reactors-and-uranium-requireme.aspx>
- [5] International Hydropower Association, 2018. [Online]. Available: <https://www.hydropower.org/>
- [6] Global Wind Energy Council, 2018. [Online]. Available: <http://www.gwec.net/global-figures/graphs/>
- [7] Boom and Bust, 2018. [Online]. Available: [https://endcoal.org/wp-content/uploads/2018/03/BoomAndBust\\_2018\\_r4.pdf](https://endcoal.org/wp-content/uploads/2018/03/BoomAndBust_2018_r4.pdf)
- [8] International Technology Roadmap for Photovoltaic Results 2017, 9th ed., Fig. 41, 2018. [Online]. Available: <http://www.itrpv.net/>
- [9] M. A. Green and R. B. Godfrey, "MIS solar cell—General theory and new experimental results for silicon," *Appl. Phys. Lett.*, vol. 9, pp. 610–612, 1976.
- [10] A. W. Blakers and M. A. Green, "678 mV open circuit voltage silicon solar cell," *Appl. Phys. Lett.*, vol. 39, pp. 483–485, 1981.
- [11] A. W. Blakers *et al.*, "18% efficient terrestrial silicon solar cell," *IEEE Electron Device Lett.*, vol. EDL-5, no. 1, pp. 12–13, Jan. 1984.
- [12] M. A. Green, A. W. Blakers, S. Jiquan, E. M. Keller, and S. R. Wenham, "19.1% efficient silicon solar cell," *Appl. Phys. Lett.*, vol. 44, pp. 1163–1165, 1984.
- [13] A. W. Blakers and M. A. Green, "20% efficient silicon solar cell," *Appl. Phys. Lett.*, vol. 48, pp. 215–217, 1986.
- [14] R. Sinton, Stanford University, private communication, 1988.
- [15] A. W. Blakers *et al.*, "22.6% efficient silicon solar cells," in *Proc. 4th Int. Photovolt. Sci. Eng. Conf.*, Sydney, Australia, Feb. 1989, pp. 801–806.
- [16] A. W. Blakers, A. Wang, A. M. Milne, J. Zhao, and M. A. Green, "22.8% efficient silicon solar cell," *Appl. Phys. Lett.*, vol. 55, pp. 1363–1365, 1989.
- [17] A. W. Blakers *et al.*, "23% efficient silicon solar cell," in *Proc. 8th Eur. Photovolt. Sol. Energy Conf. Exhib.*, Freiburg, Germany, Sep. 1989, pp. 328–329.
- [18] M. A. Green *et al.*, "Characterization of 23-percent efficient silicon solar cells," *IEEE Trans. Electron Devices*, vol. 37, no. 2, pp. 331–336, Feb. 1990.
- [19] J. Zhao, A. Wang, P. P. Altermatt, S. R. Wenham, and M. A. Green, "24% efficient PERL silicon solar cell: Recent improvements in high efficiency silicon cell research," *Sol. Energy Mater. Sol. Cells*, vols. 41/42, pp. 87–99, 1996.
- [20] J. Zhao, A. Wang, M. A. Green, and F. Ferrazza, "19.8% efficient "honeycomb" textured multicrystalline and 24.4% monocrystalline silicon solar cells," *Appl. Phys. Lett.*, vol. 73, pp. 1991–1993, 1998.
- [21] J. Zhao, A. Wang, and M. A. Green, "24.5% efficiency silicon PERT cells on MCZ substrates and 24.7% efficiency PERL cells on FZ substrates," *Prog. Photovolt.: Res. Appl.*, vol. 7, pp. 471–474, 1999.
- [22] M. A. Green, "The path to 25% silicon solar cell efficiency: History of silicon cell evolution," *Prog. Photovolt.: Res. Appl.*, vol. 17, pp. 183–189, 2009.
- [23] M. A. Green, "The passivated emitter and rear cell (PERC): From conception to mass production," *Sol. Energy Mater. Sol. Cells*, vol. 143, pp. 190–197, 2015.
- [24] E. Yablonovitch, T. Gmitter, R. M. Swanson, and Y. H. Kwark, "A 720 mV open circuit voltage SiO<sub>x</sub>:c-Si:SiO<sub>x</sub> double heterostructure solar cell," *Appl. Phys. Lett.*, vol. 47, pp. 1211–1213, 1985, doi: [10.1063/1.96331](https://doi.org/10.1063/1.96331).
- [25] A. Cuevas, "The early history of bifacial solar cells," in *Proc. 20th Eur. Photovolt. Sol. Energy Conf.*, 2005, pp. 801–805.
- [26] Y. Chevalier and I. Chambouleyron, "Getting more power out of silicon," in *Proc. 1st Eur. Commission Conf. Photovolt. Sol. Energy*, 1977, pp. 977–986.
- [27] A. Luque, J. M. Ruiz, A. Cuevas, J. Eguren, and J. M. Gomez-Agost, "Double-sided solar cells to improve static concentration," in *Proc. 1st Eur. Conf. Photovolt. Sol. Energy*, Sep. 1977, pp. 269–277.
- [28] A. Cuevas, A. Luque, J. Eguren, and J. del Alamo, "High efficiency bifacial back surface field solar cells," *Sol. Cells*, vol. 3, no. 4, pp. 337–340, 1981.
- [29] J. Knobloch, A. G. Aberle, W. Warta, and B. Voss, "Dependence of surface recombination velocities at silicon solar cell surfaces on incident light intensity," in *Proc. 8th Eur. Photovolt. Sol. Energy Conf.*, Florence, Italy, May 1988, pp. 1165–1170.
- [30] R. Hezel and K. Jaeger, "Low-temperature surface passivation of silicon for solar cells," *J. Electrochem. Soc.*, vol. 136, pp. 518–523, 1989.
- [31] A. Hübner, A. G. Aberle, and R. Hezel, "Novel cost-effective bifacial silicon solar cells with 19.4% front and 18.1% rear efficiency," *Appl. Phys. Lett.*, vol. 70, pp. 1008–1010, 1997.
- [32] R. A. Sinton, Y. Kwark, J. Y. Gan, and R. M. Swanson, "27.5-percent silicon concentrator solar cells," *IEEE Electron Device Lett.*, vol. EDL-7, no. 10, pp. 567–569, Oct. 1986.
- [33] P. Verlinden, R. A. Sinton, and R. M. Swanson, "High efficiency large area back contact concentrator solar cells with a multilevel interconnection," *Int. J. Sol. Energy*, vol. 6, pp. 347–366, 1988.
- [34] R. R. King, R. A. Sinton, and R. M. Swanson, "Doped surfaces in one sun, point contact solar cells," *Appl. Phys. Lett.*, vol. 54, pp. 1460–1462, 1989.



- [35] R. A. Sinton and R. M. Swanson, "Simplified backside-contact solar cells," *IEEE Trans. Electron Devices*, vol. 37, no. 2, pp. 348–352, Feb. 1990.
- [36] A. Cuevas, R. A. Sinton, N. K. Midkiff, and R. M. Swanson, "26-percent efficient point-junction concentrator solar cells with a front metal grid," *IEEE Electron Device Lett.*, vol. 11, no. 1, pp. 6–8, Jan. 1990.
- [37] K. A. Münzer *et al.*, "Rear side passivated and locally contacted solar cells with laser diffused selective emitter," *Energy Procedia*, vol. 15, pp. 1–9, 2012.
- [38] T. Dullweber and J. Schmidt, "Industrial silicon solar cells applying the passivated emitter and rear cell (PERC) concept—A review," *IEEE J. Photovolt.*, vol. 6, no. 5, pp. 1366–1381, Sep. 2016.
- [39] J. Liu, Y. Yao, S. Xiao, and X. Gu, "Review of status developments of high-efficiency crystalline silicon solar cells," *J. Phys. D: Appl. Phys.*, vol. 51, 2018, Art. no. 123001.
- [40] J. Schmidt, R. Peibst, and R. Brendel, "Surface passivation of crystalline silicon solar cells: Present and future," *Sol. Energy Mater. Sol. cells*, vol. 187, pp. 39–54, 2018.



**Andrew Blakers** received the B.Sc. degree from Australian National University, Canberra, ACT, Australia, in 1978, and the Ph.D. degree from the University of New South Wales, Sydney, NSW, Australia, in 1984.

He is a Professor of Engineering with Australian National University. He was a Humboldt Fellow and has held Australian Research Council QEII and Senior Research Fellowships. His research interests include silicon photovoltaic solar cells and renewable energy systems.

He is a Fellow of the Academy of Technological Sciences and Engineering, the Institute of Energy, and the Institute of Physics. He is a Public Policy Fellow at the Australian National University.